Available online at www.sciencedirect.com
ScienceDirect
Earth and Planetary Science Letters 249 (2006) 307–325
EPSL
www.elsevier.com/locate/epsl

Climate and vegetation changes 180,000 to 345,000 years ago recorded in a deep-sea core off Portugal

K.H. Roucoux [a,*], P.C. Tzedakis [a], L. de Abreu [b], N.J. Shackleton [b]

[a] *Earth and Biosphere Institute, School of Geography, University of Leeds, Leeds, LS2 9JT, United Kingdom*
[b] *Godwin Laboratory, Department of Earth Sciences, University of Cambridge, New Museums Site, Pembroke Street, Cambridge, CB2 3SA, United Kingdom*

Received 16 December 2005; received in revised form 3 July 2006; accepted 6 July 2006
Available online 22 August 2006
Editor: H. Elderfield

Abstract

A new high-resolution combined marine proxy-pollen sequence from the Portuguese margin, MD01-2443, enables direct comparison of ocean and ice volume changes with vegetation development in south-west Iberia during marine isotope stages (MIS) 7, 8 and 9. Changes in sea surface conditions on both orbital and millennial time scales are closely mirrored by forest extent, indicating a coherence of climate variability between the North Atlantic and south-west Iberia. Deglacial warming at the start of MIS 7 and 9 was interrupted by incursions of subpolar water masses at the site, accompanied by reversals in tree population expansion. During MIS 7e and 9e, the close relationship in timing and amplitude between vegetation and offshore conditions broke down: early forest collapse points to pronounced cooling and aridification on land which, although not accompanied by a change in water masses at the Portuguese margin, appears to have coincided with abrupt decreases in atmospheric methane concentration recorded in Antarctic ice cores. The most extreme glacial conditions of MIS 8 occurred during the early part, followed by an interval of warmer conditions and tree population expansion ~ 263 ka. This has sometimes been considered as indicating an early deglaciation, but the data presented here show that it was distinct from Termination III, which occurred later, in line with Milankovitch forcing. A sub-orbital oscillation in both isotopic and pollen records is observed at the end of MIS 7 (*ca.* 184 ka) which appears to be coeval with a recently identified sea level high stand.

Keywords: North Atlantic; Portugal; marine palynology; MIS 7; MIS 8; MIS 9; land-ocean correlation

1. Introduction

The pattern of vegetation development in southern Europe during the last 450 ka is well known from the long pollen records that have been produced in sedimentary sequences from Greece [1,2], Italy [3] and France [4,5] over the last 40 years (Fig. 1). In contrast to the majority of sequences from northern Europe, these sites contain continuous records spanning multiple climatic cycles. As such they provide an opportunity to study the responses of vegetation to different combinations of environmental boundary conditions at individual sites. The sequences reveal a pattern of forested intervals alternating with periods characterized by more open vegetation which, varying on time scales of 10^4 to 10^5 years, represent a response to the Milankovitch-

* Corresponding author.
E-mail address: k.roucoux@geog.leeds.ac.uk (K.H. Roucoux).

0012-821X/$ - see front matter © 2006 Elsevier B.V. All rights reserved.
doi:10.1016/j.epsl.2006.07.005

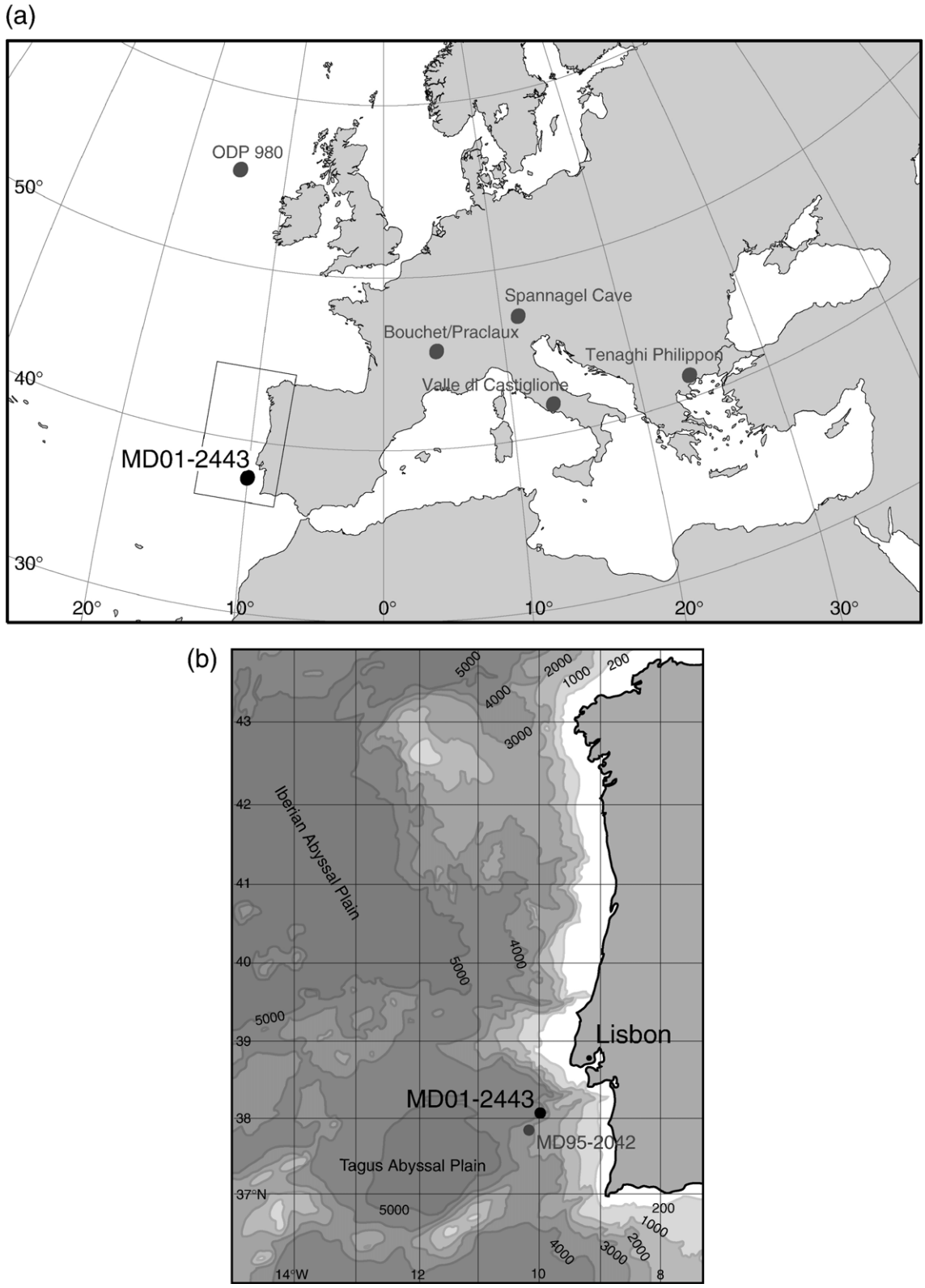

Fig. 1. (a) Location of sites discussed in the text and key European pollen sites spanning the interval 180 to 350 ka [1–5,55,72]. (b) Bathymetry of the Portuguese margin and location from which core MD01-2443 was retrieved: 37°52.8′N, 10°10.57′W at water depth 2925 m.

driven global climatic changes recorded in marine isotope records of global ice volume [6,7]. However, dating uncertainties mean that it has not been possible to determine the relationship between changes preserved in marine and terrestrial records with precision. Previous correlations have had to assume synchroneity between vegetational shifts and some feature of the marine record. For example, the correlation scheme of [8] aligned four long pollen records from southern Europe to the SPECMAP benthic $\delta^{18}O$ stack by assuming synchroneity between forest expansion and deglaciation. In doing so, this study confirmed the broad equivalence of terrestrial and marine signals and demonstrated that the marine isotope stratigraphy is a suitable framework within which to interpret terrestrial environmental records. It is also suggested that the forested intervals, previously assumed to be of similar duration, may have varied in length from one stage to another. However, the assumption of synchroneity remained to be tested.

Deep ocean sediment cores drilled close to continental margins provide a solution to the problems inherent in correlating land and ocean sequences and provide a means to test and fine-tune previous assumptions about their temporal relationship. Combining the potential for high resolution benthic and planktonic foraminiferal oxygen isotope data with pollen data in the same sediment core, such sequences record the precise relationship between the marine isotope records of ice volume and sea surface temperature, and vegetation development on land. At the Portuguese margin sedimentation rates are high enough (up to 10 cm per 1000 years [9]) to allow identification of phase offsets at centennial to millennial scales. Pollen analysis of marine cores from the Portuguese margin have already provided detailed records of vegetation development in Iberia and its relationship to the marine isotope record and to oceanographic changes in the North Atlantic for the last climatic cycle [9–12]. Work on the last interglacial in core MD95-2042 demonstrated that the boundaries of the marine-defined isotopic Last Interglacial (MIS 5e) do not coincide with the boundaries of the terrestrially-defined palynological Last Interglacial (Eemian) which began *ca.* 6 ka after Termination II and ended well into MIS 5d, *ca.* 5 ka after northern hemisphere ice sheet accumulation had begun [9–12]. This illustrated the importance of centennial to millennial scale climatic events, in determining the pattern of vegetation change at the south-west European margin, relative to the longer term forcing effects of insolation and global ice volume. In addition, our previous publication on core MD01-2443 showed that offset between marine isotopic warm stages and forested, temperate intervals on land was also characteristic of earlier interglacial complexes, and that the precise extent of the offset is variable from one warm stage to the next [13], suggesting that the factors controlling the duration of forested intervals are not a straightforward function of insolation or ice volume forcing and are still poorly understood. In this paper we present the detailed pollen stratigraphy of MD01-2443 alongside benthic and planktonic isotope data and polar foraminifera abundance from the same sediment sequence. *In situ* correlation enables the establishment of the nature and timing of the vegetation response to climate and oceanographic changes and thus the determination of the effect of abrupt (centennial to millennial scale) events and orbital scale forcing on the vegetation of south-west Europe during MIS 7, 8 and 9 (180 to 345 ka). Since there are no terrestrial sequences in Portugal reaching this far back in time, this sequence also contributes a missing piece to the picture of vegetation change across southern Europe during the Middle Pleistocene.

2. Site description

2.1. Core site

Core MD01-2443 was recovered in 2001 using a CALYPSO Giant Piston corer aboard the French research vessel *Marion Dufresne II*. The core site is located at 37° 52.85′ N, 10° 10.57′ W, 100 km south-west of Lisbon, close to the site of MD95-2042 [9,10], at a water depth of 2925 m (Fig. 1). The core is 29.48 m long and the sediments are dominated by deep ocean clay with planktonic and benthic foraminifera and a terrestrial component which includes pollen. Benthic oxygen isotope stratigraphy indicates sedimentation over the last 420,000 years with no hiatuses or erosional events [14]. Surface circulation on the Iberian margin today is southward during the summer [15] when northerly winds result in upwelling. During the rest of the year a warm undercurrent, the Portuguese Coastal Counter Current, flows northward bringing warm saline water to the region [16]. At times during the last glaciation, the North Atlantic Polar Front was situated at the latitude of southern Iberia [17,18] and icebergs reached the area during Heinrich events [19,20].

2.2. Pollen transport

Previous studies show that pollen assemblages from continental margin sediments represent vegetation

growing on the adjacent continent and that rivers, when present, tend to constitute the dominant transport vector [21,22]. The River Tagus (Tejo) flows into the North Atlantic at Lisbon and its catchment is thought to represent the main pollen source area [10]. Wind transport probably plays a relatively minor role since the prevailing winds blow from the north and west over open ocean, although the presence of a few *Cedrus* grains, presumably from North Africa [10,23], suggests a minor wind-blown component. In Portuguese margin sequences the coherence of pollen and marine isotope signals, and similarity of the pollen signal to Greenland ice core records of rapid climatic oscillation during the last glaciation [24,25], argue strongly against significant reworking or delay in incorporation of pollen into the sediment. Furthermore, from comparison of late glacial and early Holocene marine pollen records off Porto [24] with a sequence from the Serra da Estrella in central Portugal [26] it is clear that although over-representation of *Pinus* (e.g. [27]) and herbaceous pollen causes the proportions to be different, the marine pollen record faithfully reproduces patterns recorded on land [28]. Arboreal pollen (AP) percentages (excluding *Pinus*) in early Holocene deep ocean sediments are, at 40% [28,29], much lower than the 80% interpreted to represent forest cover in terrestrial records of the same age [26]. Marine AP also reaches *ca*. 40% during previous interglacials and thus the mid-points in the most rapid AP rises, which occur around 20% AP, are taken to represent the onset of forested intervals [13].

2.3. Modern climate and vegetation

The River Tagus runs north-east to south-west across the centre of the Iberian Peninsula and its catchment encompasses the north–south division between temperate and Mediterranean vegetation types at around 40°N. Today mean annual precipitation ranges from 600 mm in the lowlands to 2000 mm in the mountains which are influenced by depression-bearing westerly air-flow. Mean temperatures are 10–12 °C in January and 20–24 °C in July [30]. The Atlantic climate favours the growth of deciduous *Quercus* species: *Q. robur* is widespread at low altitudes, with *Q. pyrenaica* dominant higher up [31]. Towards the east and south, the climate becomes more Mediterranean in character with mild winters, hot, dry summers, and annual precipitation below 600 mm per year. Evergreen *Quercus* woodlands, including *Q. ilex*, *Q. rotundifolia* and *Q. coccifera*, dominate here [32,33]. *Pinus* is also important in the Iberian landscape, and *P. pinaster* dominates humid, coastal hills, particularly on the acid, siliceous soils and sands of coastal areas [31]. Shrub communities are characterized by ericaceous heath on the Atlantic coasts and hills, especially on acidic substrates, while evergreen aromatic shrubs dominate in drier areas [31].

3. Materials and methods

3.1. Stable isotopes

Stable isotope analyses were carried out using a VG PRISM mass spectrometer (for all benthic measurements and a few very small samples of planktonics) or a VG SIRA mass spectrometer (for the majority of planktonic measurements). On both instruments the samples are reacted sequentially using ISOCARB systems. For the planktonic record about 25 specimens of *Globigerina bulloides* were selected from a sieved size fraction 355–425 μm. For the benthic record several different species were used as no single species was present in sufficient numbers to generate a continuous record. Where possible two or three separate analyses of different species were made in each sample; a correction factor was applied according to the species and the average of all the corrected values at each level is shown in the figures. The following species were analysed, and adjusted as indicated: *Cibicidoides robertsonianus*, +0.50; *Uvigerine peregrina* and similar specimens, *0.0*; *Globobulimina affinis*, −0.30; *Cibicidoides wuellerstorfi*, +0.64; *Cibicidoides kullenbergi*, +0.54; *Hoegludina elegans*, −0.60; *Oridorsalis umbonatus*, 0.0; *Cassidulina carinata*, 0.0. These adjustments are optimised for cores in this area in accordance with the long-standing convention by which *Uvigerina perigrina* is assumed to deposit oxygen in isotopic equilibrium [34]. Out of about 700 measurements 12 were rejected as significantly discrepant and in addition one sample level (19.38 m) was rejected because of very wide scatter among the four measurements. For the remaining 213 replicated samples, the average estimated standard deviation is 0.07‰.

3.2. Foraminiferal faunal analysis

The sediment fraction larger than 150 μm was divided by microsplitter to obtain 300 to 500 specimens of planktonic foraminifera per sample. They were counted and identified following [35] and [36]. Only the proportion of left-coiling *Neogloboquadrina pachyderma* (*N. pachyderma* s.) in the total planktonic fauna is presented here.

3.3. Palynological analysis

Sub-samples of 4 cm^3, at intervals of between 2 and 8 cm, were prepared for pollen analysis using a standard hot acid digestion technique [37]. Identification was carried out using reference material and [38]. Nomenclature follows *Flora Europaea* [39]. Pollen abundance is presented as percentages of a sum which excludes *Pinus*, Pteridophyte spores and aquatic taxa. A minimum of 150 pollen grains, excluding *Pinus*, aquatics and spores, was counted in each of 214 samples. *Quercus* pollen was divided into deciduous and evergreen morphotypes. The deciduous *Quercus* type includes *Q. robur*, *Q. petrea* and *Q. suber*, while the evergreen *Quercus* type includes *Q. ilex*, *Q. coccifera* and *Q. rotundifolia*. Preservation was not sufficiently good to allow routine subdivision of Ericaceae, but some taxa can be eliminated on the basis of those features that are preserved well. Neither *Arbutus unedo* nor *Erica umbellata* were encountered. *Erica arborea* may be present. The small size, triangular tetrad shape and long colpi of many grains suggest that they could represent *Erica erigena* [40].

3.4. Statistical analyses

Cluster analysis was carried out on the pollen dataset in order to identify recurring groups of taxa which may represent vegetation communities. Samples were grouped using Ward's linkage method and the Chi-squared distance measure [41]. All taxa present at >3% in more than one sample are included, except *Pinus*. The species that characterize samples in each group were identified by indicator species analysis [42].

The pollen sequence is divided into zones (*sensu* [43]) with the aid of numerical zonation using constrained cluster analysis (CONISS) in the pollen plotting and analysis program PSIMPOLL. The zones are illustrated in Fig. 3 and their main features described in Table 2.

3.5. Chronology

The time scale for MD01-2443 [13] was developed by aligning the benthic $\delta^{18}O$ record to the Antarctic Vostok deuterium (D/H) record [44]. This was based on the study by [45] which showed strong similarity between the benthic $\delta^{18}O$ record off Portugal and Antarctic temperatures. The implication that shifts in benthic $\delta^{18}O$ are synchronous with shifts in Antarctic temperature allows the use of chronologies developed for the Antarctic ice cores to generate an age model for MD01-2443. The Vostok time scale used here has been developed by F. Parrenin (personal communication) through alignment with the EPICA Dome C record [46]. It is considered an improvement on the Vostok glaciological time scale (GT4) of [44] because ice at the Vostok site originates upstream, where accumulation changes are poorly constrained, whereas ice at Dome C accumulates *in situ*, which facilitates derivation of a time scale based on an ice-flow model. Fig. 2 shows the alignment of the MD01-2443 record to Vostok D/H and the resulting sediment accumulation rates (SAR). Inflections of the SAR curve show the location of the control points (listed in Table 1), which were chosen at the mid-points of cold to warm transitions between marine isotopic stages. The greatest source of uncertainty in this age model is that associated with the Vostok chronology where the age uncertainty, between MIS 5.5 and MIS 11, is ±6 ka (at 2σ), which is equal to the size of the orbital control windows used to constrain the age of glacial terminations in the development of the ice core chronology ([46]; F. Parrenin, personal communication). The maximum age uncertainty arising from visual correlation of MD01-2443 benthic $\delta^{18}O$ and Vostok D/H is 300 years, that is equivalent to half the longest sampling interval across the cold-warm transitions (whose mid-points were used as tie-points). When the uncertainties on the ice core chronology and the maximum visual correlation uncertainty are summed in quadrature (according to convention) the latter become insignificant (for example, the resulting confidence interval at termination III is ±6.007 ka). Another, potentially large, source of age uncertainty is in the assumption of synchrony between Vostok D/H and MD01-2443 benthic $\delta^{18}O$. Since our age model

Table 1
Age control points established by comparison of benthic $\delta^{18}O$ in MD01-2443 with Vostok D/H record (F. Parrenin, unpublished data)

Depth in MD01-2443 (m)	Age (ka)
16.34	183.5
16.46	185.3
16.58	187.45
17.18	201.00
18.38	216.80
19.32	244.45
19.44	248.15
20.5	266.50
21.96	290.30
22.78	305.68
23.28	316.54
24.68	338.00

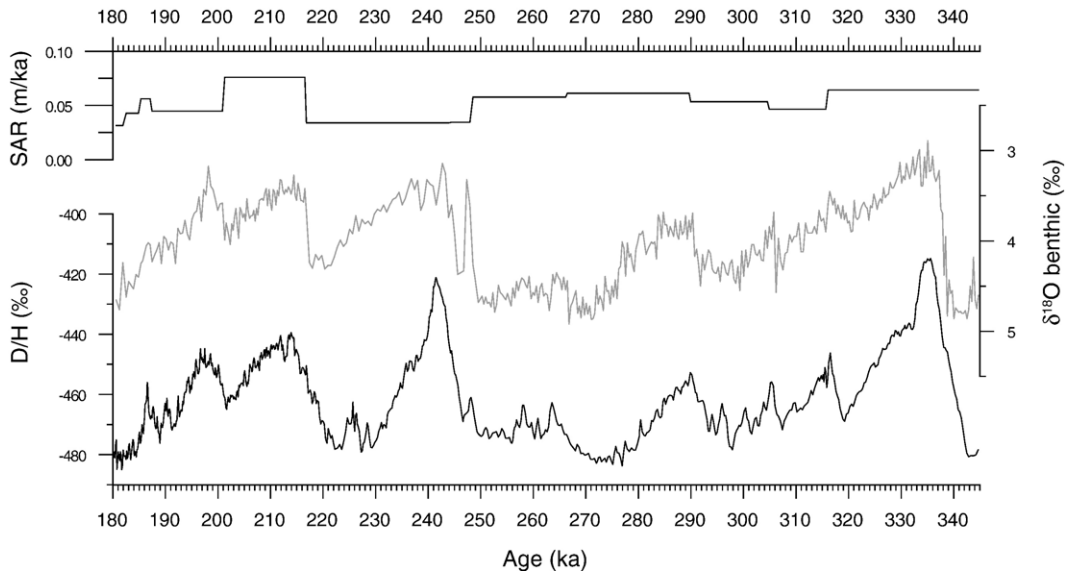

Fig. 2. Basis of the age model for MD01-2443. Age control was established by alignment of the MD01-2443 benthic foraminiferal oxygen isotope record (δ^{18}O (‰) shown in grey) to the Vostok deuterium record (D/H (‰) shown in black) [44]. Inflections of the sediment accumulation rate (SAR) curve indicate positions of the tie points.

rests on this assumption, we do not incorporate this in the quantification of confidence intervals.

4. Results and interpretation

4.1. Stable isotopes

The benthic δ^{18}O record (Figs. 2 and 3) shows the classic succession of climatic cycles representing the accumulation and wasting of continental ice masses through MIS 7, 8, 9 and the early part of MIS 6. Rapid shifts to lighter benthic δ^{18}O values at the MIS 7/8 boundary and at the MIS 9/10 boundary represent Terminations III and IV (TIII and TIV), respectively [47]. The interglacial complexes MIS 7 and 9 are resolved into three warm, low ice volume episodes (substages a, c and e) and two intervening cold intervals of greater ice volume (substages b and d). MIS 8 is resolved into two distinct periods of larger ice volume separated by a period of lower ice volume which contains marine isotope event 8.3 [48]. Here we refer to this interval of lower ice volume, between 253 ka and 266 ka, as MIS 8c. Sub-orbital scale oscillations are also recorded: MIS 9c is interrupted by an isotopically heavier interval and, at the end of MIS 7, there is an additional light peak in the planktonic δ^{18}O which coincides with a shoulder or pause in the trend of increasingly heavy benthic δ^{18}O, following the main peak of MIS 7a.

Previous studies have suggested that planktonic δ^{18}O at the Portuguese margin is most strongly influenced by sea surface temperature with salinity having a relatively small impact on the signal [18,49,50]. This is supported by the close correspondence of the planktonic δ^{18}O signal and sea surface temperature estimates based on faunal analysis of planktonic foraminifera (L. de Abreu, in prep.). There is a temporal offset between the benthic and planktonic δ^{18}O signals in this sequence, which is particularly pronounced at deglaciations: the shift to lighter values is recorded 3000 years earlier at MIS 7/8 and 1000 years earlier at MIS 9/10. There is also a pronounced offset at MIS 8c, with relatively light planktonic δ^{18}O values beginning later, at 265 ka, and ending later, at 247 ka. The differences in timing may be partly due to changes in deep water temperatures and δ^{18}O, reflecting changes in deep-water hydrography as has been shown for Termination I [51].

4.2. Polar foraminifera

The most pronounced peaks in *N. pachyderma* s. abundance (Fig. 3), as a percentage of total planktonic foraminifera, reach between 40 and 50% during the deglaciations (coinciding with TIII and TIV) and during the early part of MIS 8 (between 268 and 264 ka, which we refer to as MIS 8d) when benthic δ^{18}O values record extremely large ice volume and planktonic δ^{18}O values indicate low sea surface temperatures. This species is considered as an indicator of the development of sub-polar surface water conditions [50].

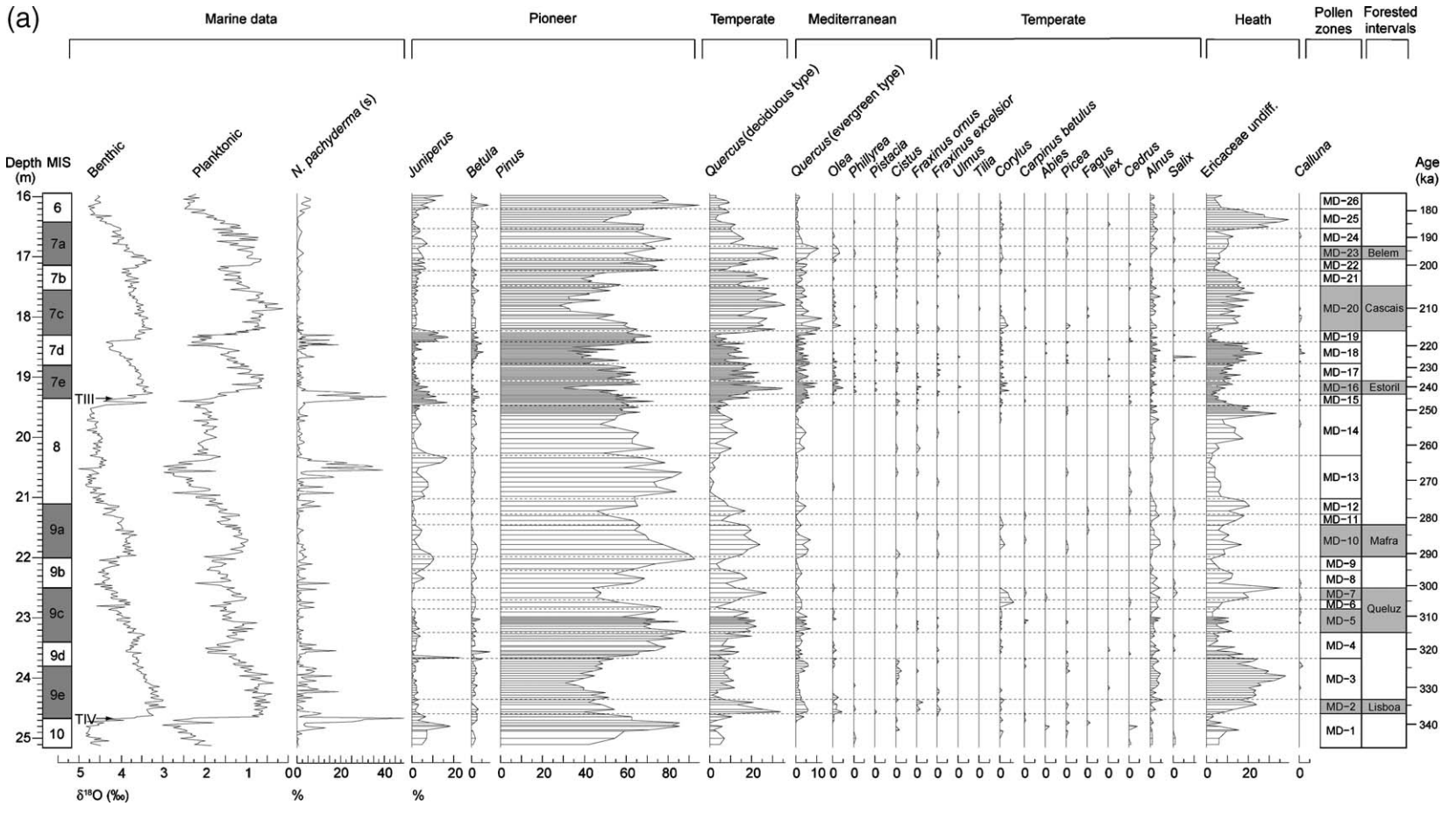

Fig. 3. Percentage pollen and marine proxy data for MD01-2443 plotted against depth. (a) Pioneer, temperate, Mediterranean and heath vegetation. (b) Steppe taxa, ubiquitous herbs, aquatic taxa and Pteridophytes. Pollen assemblage zones are shown on the right and forested intervals, where arboreal pollen percentage is above 20 % [13], are shaded in grey and assigned stage names.

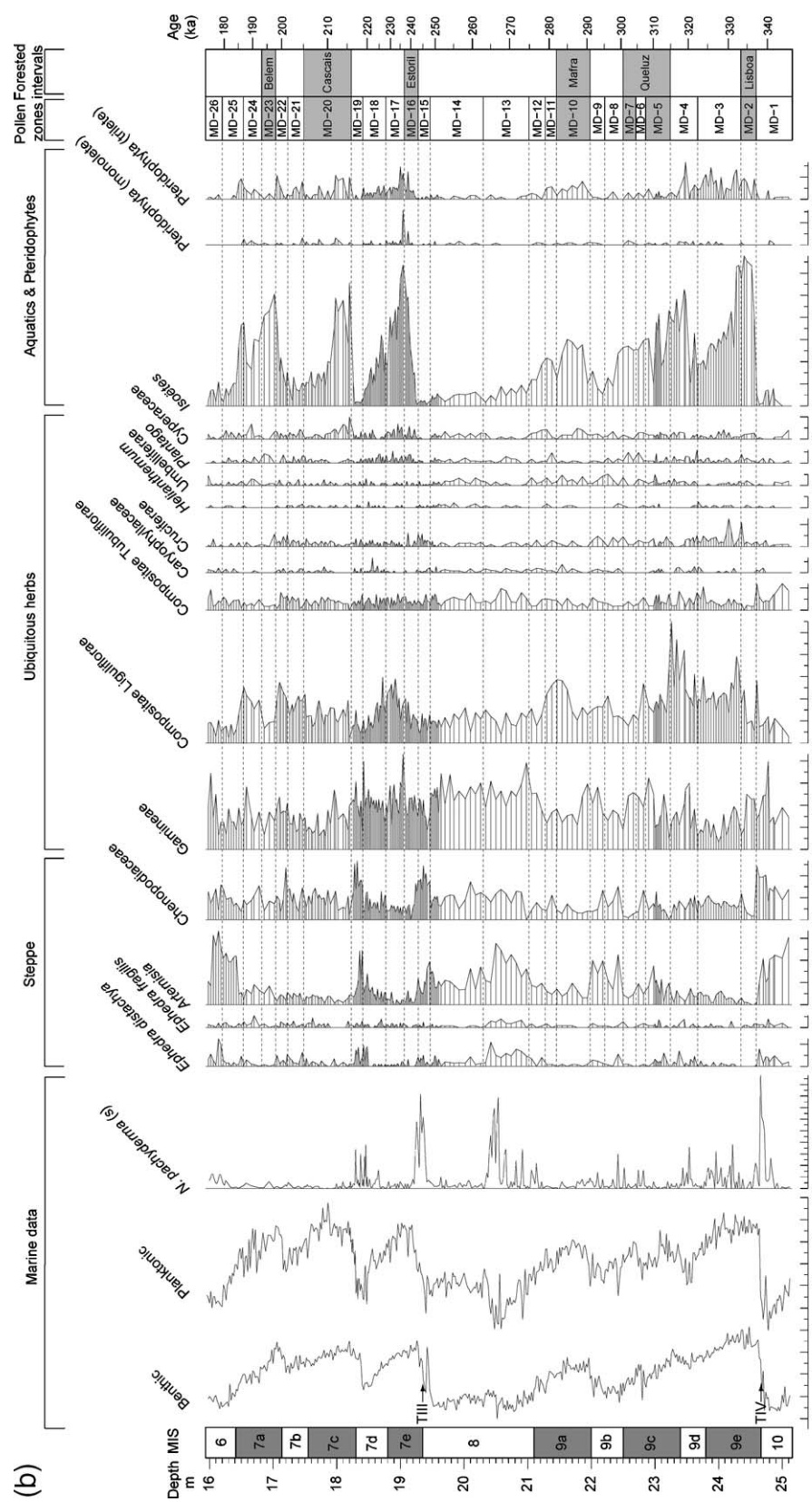

Fig. 3 (*continued*).

4.3. Palynology

Results of palynological analyses are presented as percentage pollen diagrams (Fig. 3a and b) and summarized in Table 2. Deciduous *Quercus* is the dominant temperate tree taxon (reaching maximum values of 35%). Pollen of other temperate trees is present in much smaller quantities, the most abundant being *Corylus* and *Alnus*. *Ulmus*, *Carpinus*, *Fagus* and *Abies* are represented by occasional grains. The most abundant Mediterranean tree taxa are evergreen *Quercus*, and *Olea*. Other Mediterranean taxa, *Pistacia*, *Fraxinus ornus*, and *Phillyrea*, are present in much smaller quantities. *Pinus* pollen is very abundant, but is known to be consistently over-represented in marine pollen records. The most abundant herbaceous taxa are Ericaceae, Gramineae, the steppe taxa *Artemisia* and Chenopodiaceae, pollen of the type Compositae Liguliflorae, and the spores of *Isoëtes hystrix*.

4.4. Cluster analysis

A scheme of five cluster groups provides an informative summary of the pollen data. Each cluster represents a set of co-occurring taxa, that can be interpreted as broad vegetation types (Table 3). The occurrence of these groups is plotted stratigraphically, above planktonic δ^{18}O, in Fig. 4. A repeating pattern (or succession) of vegetation types is evident and shows a clear correspondence to the progression of precessional scale climatic cycles indicated here by the planktonic δ^{18}O curve.

4.5. Vegetation changes during MIS 7, 8 and 9

4.5.1. MIS 9

Afforestation in south-west Portugal associated with TIV began with *Juniperus* and *Pinus*, followed by deciduous *Quercus ca.* 1000 years after the shift to light planktonic isotope values. A peak in *N. pachyderma* s. percentages indicates the presence of sub-polar water masses offshore at the termination and interruptions in forest expansion indicate coeval cooling and drying on land. Temperate tree populations expanded abruptly as soon as cold waters retreated at 336 ka. Deciduous *Quercus* dominated in the earliest phase (336.5–333 ka) accompanied by evergreen *Quercus* and *Olea*. The *Quercus* phase ended abruptly within the isotopic plateau making the forest interval, Lisboa (MD-2), short (3.6 ka) compared with the duration of MIS 9e (14 ka). After a brief maximum in herbaceous taxa (mainly Compositae Liguliflorae), Ericaceae expanded to a peak at 327 ka, and temperate tree populations recovered slightly. This was followed by a pronounced decline as sea surface temperatures fell and global ice volume increased.

MIS 9d is characterized by relatively minor excursions in benthic and planktonic isotope values and moderate influence of sub-polar water masses. Herbaceous vegetation was dominated by grass with a relatively small contribution by steppe communities. This suggests a less arid and cold climate than during stadial intervals where steppe was more abundant and temperatures offshore were lower.

Planktonic δ^{18}O records two clear warm intervals (though not as warm as MIS 9e) with a cooler phase in between during MIS 9c. This is clearly reflected in the pollen record which shows moderate temperate forest extent (Queluz forest interval; MD-5 to 7) interrupted by a decrease (MD-6). The second warm interval of MIS 9c (305 to 299 ka) saw greater heath expansion than the first which could indicate higher precipitation levels and a greater degree of soil deterioration.

MIS 9b corresponds to a pronounced tree population collapse coeval with a moderate and brief incursion of sub-polar water offshore and large accumulation of continental ice (more clearly recorded in other sequences; e.g. Shackleton 2000). Steppe vegetation expanded to its greatest extent since MIS 10, indicating dry, cold conditions on land.

Forest expansion at the start of MIS 9a corresponds closely with planktonic and benthic δ^{18}O and was intermediate in extent between that of 9c and 9e. Evergreen *Quercus* is the only Mediterranean taxon to make a significant contribution (Mafra forest interval; MD-10). After 276 ka, increasing ice volume and decreasing sea surface temperatures coincided with a decline in heath and forest populations, indicating cooling and drying.

4.5.2. MIS 8

Benthic δ^{18}O indicates greatest ice volume, and planktonic δ^{18}O and *N. pachyderma* s. record lowest sea surface temperature, in the early part of MIS 8 (MIS 8d). The end of MIS 8d is marked by a large peak in *N. pachyderma* s., pointing to the occurrence of a Heinrich-type event. This is followed by an interval of warmer conditions (MIS 8c) the onset of which is, in the planktonic record, close to the peak in July insolation at 65°N [52] (Fig. 5). A brief return to low temperatures is recorded before Termination III. Portuguese vegetation reflects this pattern, with extensive steppe vegetation and reduced tree populations between 276.6 and 265 ka, culminating in the largest tree and heath population collapse at 265 ka, immediately following the *N.*

Table 2
The main features of the pollen record

Forest stages	Pollen zones	Main pollen features
	MD-26	High percentages of steppe (50%) and pioneer (15%) pollen. Peak in *Pinus* abundance.
	MD-25	High percentages of Ericaceae pollen (40%) near start of zone but decreases to <10% by the end. *Isoëtes* abundant at start (35%) then decreases. Steppe pollen increases through zone (reaching 30% by the end).
	MD-24	Moderate temperate tree pollen values (just under 20% deciduous *Quercus*) following a short-lived decrease. Low percentages of Mediterranean taxa. Ericaceae increases to 30% at top of zone. Peak in *Pinus* abundance. *Isoëtes* (35%) and other spores reach high values at the top.
Belem	MD-23	Temperate and Mediterranean tree pollen abundant: deciduous *Quercus* 32%, evergreen *Quercus* 12%, *Olea* 5%. Peak in *Isoëtes* (55%).
	MD-22	Chenopodiaceae, Gramineae and C. Liguliflorae each around 25%. In upper part of zone temperate tree pollen increases, peak in *Pinus* reached, and steppe abundance decreases.
	MD-21	Herbaceous pollen abundant. Ericaceae decreasing. Relatively low percentages for temperate and Mediterranean pollen.
Cascais	MD-20	Temperate and Mediterranean tree pollen abundant: deciduous *Quercus* 30%, evergreen *Quercus* 12%, *Olea* 5%, *Corylus* 5%. *Isoëtes* (55%) and other spores reach high values. Oscillation at 18 m in which tree pollen falls decrease briefly and Gramineae increases; followed by an increase in temperate (but not Mediterranean) tree pollen to 40%. Ericaceae pollen increasing throughout.
	MD-19	High percentages of steppe (50%) and pioneer (20%) pollen. Peak in *Pinus* abundance. Low values of temperate trees at start but increase at end of zone.
	MD-18	Ericaceae pollen abundant reaching a peak of 30%. Decreasing temperate trees. Increasing percentages of steppe pollen.
	MD-17	Herbaceous elements abundant: Gramineae and C. Liguliflorae both around 30%. Moderate values for temperate and Mediterranean tree pollen (largely remain <20%), and Ericaceae (around 10%).
Estoril	MD-16	Temperate and Mediterranean tree pollen abundant: deciduous *Quercus* 35%, evergreen *Quercus* 10%, Olea 5%. Continuous curve of *Corylus* begins. Decrease in tree pollen at 19.10 m, then recovers before decreasing again at end of zone. *Isoëtes* (65%) and other spores reach high values.
	MD-15	High values *Juniperus* (20%) and Chenopodiaceae (25%). Increasing deciduous *Quercus*. Decreasing steppe. Ericaceae also decreasing. Peak in *Pinus* abundance.
	MD-14	Continued increase in percentages of temperate taxa, reaching 15% with a slight increase in Mediterranean tree pollen. These fall to very low values at end of zone. Steppe pollen is reduced (ca. 20%) relative to zone below. Ericaceae increases reaching a peak of 35% in the upper part, then decrease by end of zone.
	MD-13	Steppe pollen abundant reaching 35%. *Pinus* reaches a peak in lower part of the zone, followed by an increase in *Juniperus* (to 20%) then an increase in temperate tree pollen, deciduous *Quercus* reaching 10% as *Juniperus* decreases.
	MD-12	Ericaceae pollen abundant (20%). Brief return to moderate percentages of deciduous (15%) and evergreen (5%) *Quercus*. These decrease towards end of zone while steppe and Gramineae pollen increase.
	MD-11	Low percentages of temperate and Mediterranean tree pollen. Ericaceae increasing.
Mafra	MD-10	Temperate and Mediterranean tree pollen abundant: deciduous *Quercus* 25%, evergreen *Quercus* 5% in lower half of zone. *Isoëtes* (30%) and other spores abundant. Tree pollen decreases towards top as herbaceous elements and Ericaceae increase.
	MD-9	High percentages of steppe (35%) and pioneer pollen (15%). *Pinus* peak near end of zone.
	MD-8	Decrease in deciduous *Quercus* and Ericaceae and peak in steppe taxa at 22.40 m, followed by return of *Quercus* to moderate values. Mediterranean taxa rare. Increasing abundance of *Juniperus*, steppe, C. Liguliflorae and Gramineae pollen through zone.
Queluz	MD-7	Temperate tree pollen abundant: deciduous *Quercus* reaches 25%. Ericaceae increases to a peak of 35% one sample above the *Quercus* peak. Both decrease at 22.40 m to <10% while steppe pollen increases to 45%.
	MD-6	Increase in herbaceous pollen percentages: Chenopodiaceae 15%, Gramineae 25%, C. Liguliflorae 25%. Drop in tree pollen abundance: deciduous *Quercus* falls below 5%. Peak in *Corylus* (5%) towards end of zone as deciduous *Quercus* recovers.
	MD-5	Moderate abundance of temperate and Mediterranean tree pollen: deciduous *Quercus* 22%, evergreen *Quercus* 7%. Peak in *Pinus* early in the zone. Gradual increase in steppe.
	MD-4	Herbaceous pollen abundant: Gramineae ca. 30%, C. Liguliflorae between 20 and 45%. Deciduous *Quercus* and Ericaceae remain below 10% for most part. Peak in *Isoëtes* (50%) and other spores.
	MD-3	High percentages of Ericaceae pollen which increase to a peak (40%) at 24 m then decrease, and of Compositae Liguliflorae (40%). *Isoëtes* falls from 50 to 20%.
Lisboa	MD-2	High temperate and Mediterranean tree pollen percentages: deciduous *Quercus* 35%, evergreen *Quercus* and *Olea* both 5%. *Isoëtes* attains a peak of 65%. Other spores also abundant. Increasing Ericaceae percentages.
	MD-1	Steppe (40%), Gramineae (40%), and *Juniperus* (20%) pollen abundant. *Pinus* and *Juniperus*, both increasing.

Pollen assemblage zones and names assigned to forested intervals indicated on the left (see also Table 3). Values given in brackets represent the highest percentage value attained in the zone unless indicated otherwise.

Table 3

Groups (a)	Indicator taxa (b)	Vegetation types (c)	Climate according to marine proxies (d)	Corresponding planktic δ^{18}O range (e) (‰)
A	*Ephedra distachya* (45), *Artemisia* (42), *Juniperus* (27), *E. fragilis* (24), Gramineae (24), Compositae Tubuliflorae (24)	Steppe (+pioneer)	Cold stage	1.5–3
B	Ericaceae (35), *Artemisia* (25), *Alnus* (24)	Heath (+steppe)	Late warm stage and transitions to cold stage	1.2–2
C	*Juniperus* (47), Chenopodiaceae (33)	Pioneer (+steppe)	Transitions from cold to warm stage	0.6–2.6
D	(*Isoetes* [52], Pterydophytes trilete [42]), *Olea* (38), *Corylus* (38) evergreen *Quercus* (33), deciduous *Quercus* (32) Cyperaceae (26)	Temperate woodland + Mediterranean elements	Early warm stage	0.4–1.4
E	Compositae Liguliflorae (31), deciduous *Quercus* (28), (*Isoetes* [28], Pterydophytes trilete [26]), *Alnus* (25), Ericaceae (24)	Temperate woodland+ heath	Late warm stage	0.1–1.7

(a) Groups established by cluster analysis using Ward's hierarchical linkage method and Chi-squared distance measure [41]. (b) Taxa indicative of samples in each group, identified by indicator species analysis [42]. Taxa with the highest indicator values (over 24) for each group are given in descending order. Where there is a gap of 10 or more between the indicator values for the top taxa and the next in the list, the top taxa are marked in bold to indicate which are most strongly indicative in strictly numerical terms. (c) Suggested vegetation communities represented by the clusters (dominant vegetation first, more minor vegetation in brackets). (d) Stage in marine-defined climatic cycles at which vegetation communities most often occur. (e) Range of planktonic δ^{18}O values with which vegetation communities are associated.

pachyderma s. maximum. An expansion of tree populations occurred between 265 and 252 ka, followed by a return to steppe and pioneer vegetation (252 to 246 ka) coincident with the arrival of sub-polar water masses offshore before TIII.

4.5.3. MIS 7

Temperate forest expansion at the start of the Estoril forest interval (MD-16) coincides closely with the shift in planktonic δ^{18}O to light values at the start of MIS 7e. Reversals in the trend appear to coincide with peaks in *N. pachyderma* s. and the final, most rapid, part of the expansion took place only once sub-polar waters had retreated. The forested interval was shorter (6.2 ka) than the marine isotopic warm stage (17 ka), ending mid-way through the plateau in planktonic δ^{18}O in a similar way to that of MIS 9e but it differs in that heath expanded more gradually, not dominating the vegetation until

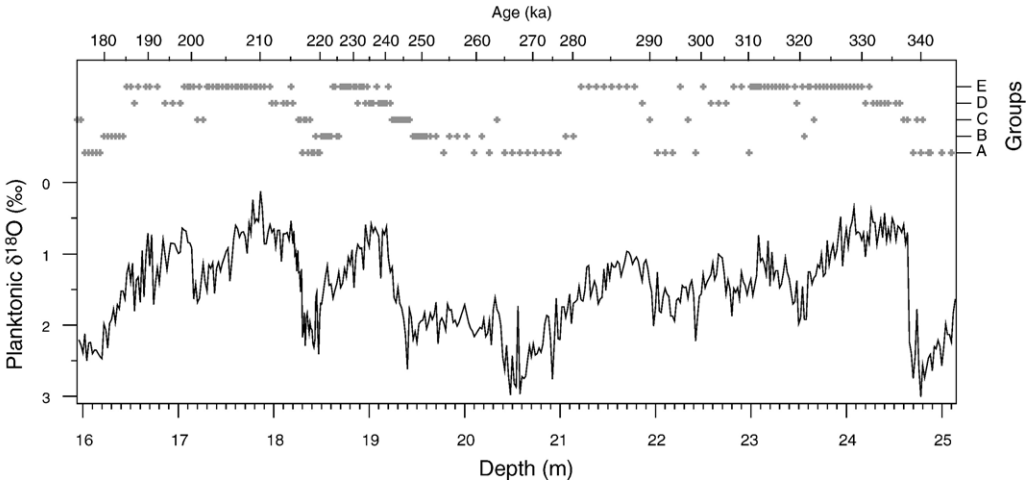

Fig. 4. Stratigraphic distribution of sample cluster membership, shown above planktonic δ^{18}O data to illustrate the succession of vegetation types through precessional climatic cycles. A — steppe (with pioneer) vegetation; B — heath (with steppe) vegetation; C — pioneer (with steppe) vegetation; D — temperate woodland and heath vegetation; E — temperate woodland with Mediterranean elements (see also Table 3).

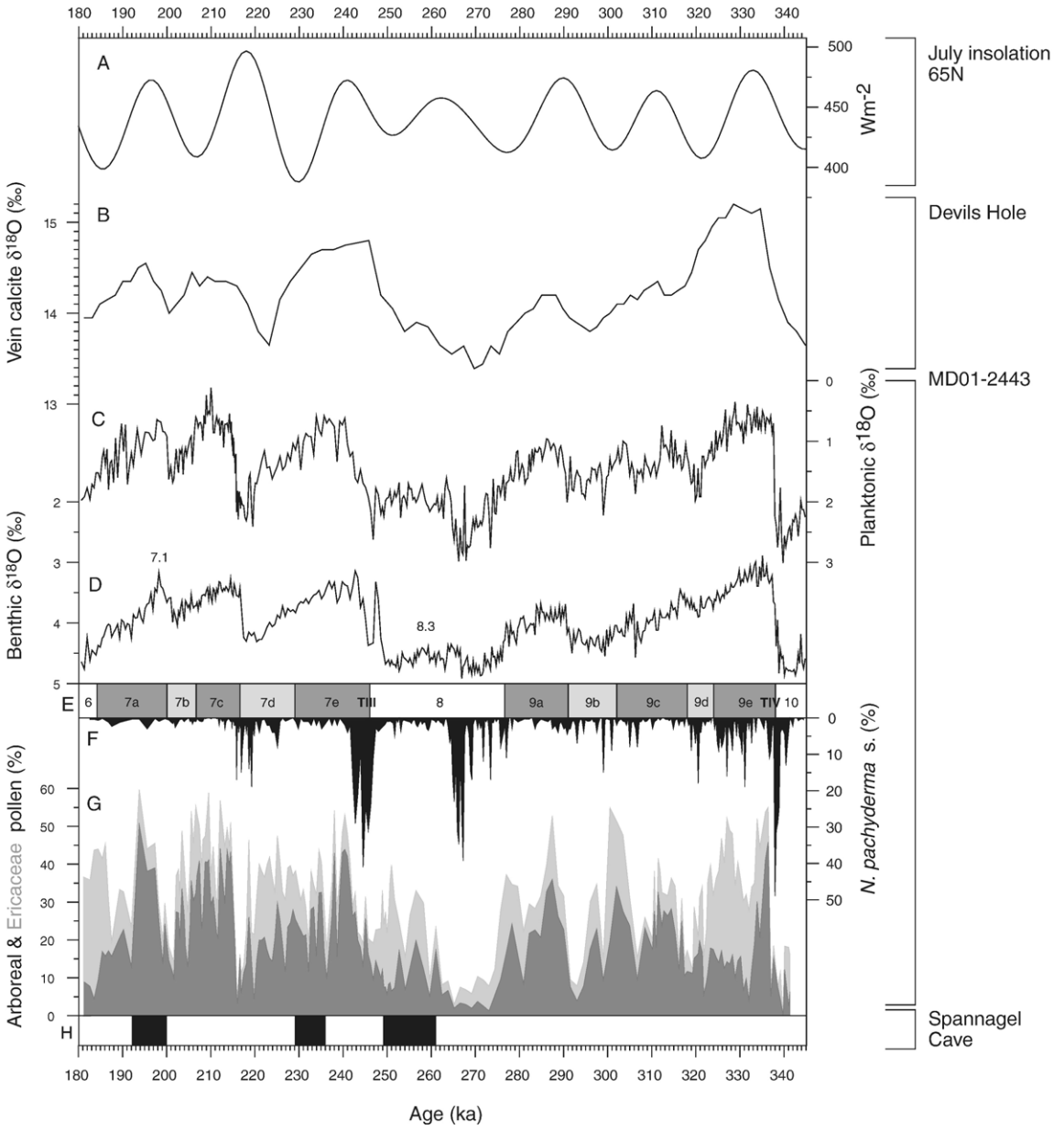

Fig. 5. Comparison of data from MD01-2443, Spannagel Cave and Devils Hole. From the top down: (A) July insolation at 65°N [53]; (B) δ^{18}O of vein calcite in Devils Hole, Nevada, plotted on U/Th time scale [72]; data from deep marine core MD01-2443 for the period 180 to 345 ka plotted on the Vostok/EPICA Dome C-derived time scale (F. Parrenin personal communication), (C) planktonic δ^{18}O, (D) benthic δ^{18}O, (E) marine isotope stratigraphy (Terminations III and IV are indicated), (F) *N. pachyderma* s. percentages, (G) cumulative percentage data for arboreal pollen and Ericaceae; (H) black bars indicate U-series dated periods of speleothem growth in Spannagel Cave (Zillertal Alps, Austria) [71].

later. The ensuing period of small but oscillating tree populations and expanding ericaceous heath coincided with falling North Atlantic sea surface temperatures and increasing global ice volume.

The pronounced contraction of tree populations and expansion of steppe vegetation coinciding with MIS 7d indicates cold, dry conditions on land, similar to the early part of MIS 8. Temperatures offshore reached glacial levels and sub-polar water masses extended to this latitude. Records from Antarctica and the North Atlantic show MIS 7d to have been an extremely cold stadial event [44,53,54], low global temperatures and large ice volume resulting from high eccentricity, low obliquity and high precession which

combined to give low northern hemisphere summer insolation [52].

Forest expansion at the start of MIS 7c, marking the beginning of the Cascais forest interval (MD-20), closely tracked planktonic δ^{18}O. This substage saw the longest forested interval of MIS 7 (10.3 ka), mirroring the duration of sea surface warmth. Mediterranean taxa and *Corylus* made a significant contribution to the vegetation only during the first 3 ka of the forested interval. At 212 ka tree populations decreased briefly, after which only deciduous *Quercus* recovered completely, reaching the greatest extent of the whole sequence. Ericaceae populations expanded throughout the period of lightest planktonic δ^{18}O, reaching a maximum at 206 ka. Heath then joined temperate tree populations in a gradual decline, coinciding with falling sea surface temperatures and increasing global ice volume.

Atlantic sea surface temperatures declined only slightly during MIS 7b [54] and sea level estimates indicate only minor accumulation of ice [55]. In MD01-2443 polar foraminifera remain rare. Of all the stadial events of this sequence, this has the least polar water influence. Steppe elements remained correspondingly rare and while temperate tree populations were small, they remained more widespread than during the other cold stages recorded here.

The first δ^{18}O peak of MIS 7a is represented by a tree population expansion which, although short-lived, is more pronounced than in the previous MIS 7 warm sub-stages, with significant contributions of Mediterranean elements (Belem forest interval). The decline in tree populations that marks the end of the forest interval was followed by a moderate re-expansion of deciduous *Quercus* (MD-23) associated with the second planktonic δ^{18}O peak of MIS 7a and a step in the benthic δ^{18}O curve. In the planktonic record this isotopically light peak is resolved into two parts, interrupted by a brief interval of heavier values, which is reflected by an oscillation in deciduous *Quercus* abundance (with one peak in MD-23 and another near the base of MD-25). Declining tree populations were then accompanied by a pronounced increase in the extent of heathland (MD-25); a phase of extensive heathland spans the MIS 7/6 transition.

4.5.4. MIS 6

The first 4 ka of MIS 6 are recorded here. Falling sea surface temperatures and increasing global ice volume coincided with shrinking forests and heathland, and the expansion of steppe and *Juniperus*, which indicate the onset of cold and dry conditions.

5. Discussion

5.1. The nature of the vegetation response

There is a clear and reasonably consistent relationship between the amplitude of oscillations in planktonic δ^{18}O and the amplitude of oscillations in arboreal pollen percentages at both orbital and millennial time scales. Concordance is also observed in the amplitude of the arboreal pollen and benthic isotope curves and with reconstructed changes in sea level. According to the sea level estimates of [55] and [56], and the direct determinations of [57], the highest sea level of MIS 9 occurred in substage 9e, which corresponds to the greatest forest extent of this stage, while the relatively lower high stands of substages 9c and 9a saw more moderate forest expansion in south-west Iberia. Differences between the high stands of MIS 7 are less pronounced: sea level appears slightly higher during sub-stage 7c in the estimates of [56], while in the reconstruction of [55], MIS 7a saw the highest sea level, although error margins on the estimates for each substage overlap. Sea level determinations from Barbados corals also suggest higher sea level during MIS 7a [58]. The largest tree population expansion in Iberia appears to have occurred during MIS 7a, although the differences in AP between the temperate sub-stages of MIS 7 are small and may not represent significant differences in tree population extent. The extensive forest and sea levels as high, or higher, than in the previous two MIS 7 substages are unexpected in light of relatively low insolation values [52] and patterns recorded in Antarctica where temperature and concentrations of carbon dioxide and methane are lower than MIS 7e and 7c [44]. A possible explanation, for the higher AP values in MIS 7a, is the persistence of relatively large tree populations through the preceding stadial MIS 7b which meant that even minor warming could subsequently have led to extensive forest [59]. Likewise, the minor ice accumulation of MIS 7b may explain the small residual ice volume, and correspondingly high sea level, of the ensuing warm substage.

The close relationship, in timing and amplitude, between AP and benthic and planktonic δ^{18}O breaks down in MIS 7e and 9e. Here, although forest initially expands in proportion to offshore warming and deglaciation, it contracts after only 3.6 ka in 9e and 6.2 ka in 7e, pointing to pronounced cooling and aridity on land. An increase in herbaceous pollen and corresponding drop in AP could be caused by a pulse of reworked glacial sediment off the shelf but neither magnetic susceptibility nor sediment density, proxies that might

indicate a change in sediment source, record any significant shift at these times [60]. In the absence of a taphonomic explanation, we interpret the drop in AP to represent a real decline in tree population extent. This forest decline is not reflected in planktonic or benthic δ^{18}O values, and it took place long before the sea surface cooling and continental ice accumulation of the ensuing stadials began. It is also not clearly reflected in the abundance of *N. pachyderma* s. (neither here nor further north in ODP 980 [54]), which we would expect to increase were the drop in AP related to a change in ocean surface conditions. During MIS 9e an increase in *N. pachyderma* s. is observed but this post-dates the drop in AP values, which suggests that a change in ocean circulation was not the proximal cause of the forest collapse. During MIS 7e, *N. pachyderma* s. values remained low throughout. Comparison with other southern European sequences [13] revealed that similar forest collapses are also recorded at *ca.* 333 ka and 237 ka, although in the MIS 9e event, forest was able to recover in France, Italy and Greece, while in Portugal heath, rather than forest, subsequently developed. In the absence of evidence for changes in North Atlantic circulation the causes of these forest collapses remain unclear. Tzedakis et al. [13], however, pointed out that these events were coeval with abrupt declines in atmospheric methane concentration, following the early interglacial overshoots observed in the Vostok record [44]. The coincidence of these changes may reflect the occurrence of a global shift in climate conditions occurring within interglacials.

Vegetation types, identified by cluster analysis, show a clear correspondence to the progression of precessional scale climatic cycles or marine isotopic substages. Extensive open steppe vegetation (cluster A) indicates cold, dry conditions on land and coincides with the lowest temperatures offshore and largest continental ice volume. Pioneer populations dominated by *Juniperus* (cluster C) expanded in response to the earliest phases of warming. Extensive temperate woodland and populations of Mediterranean trees (cluster D) characterize the early phase of peak warmth offshore. Contraction of tree populations and expansion of ericaceous heath (cluster E) follow through the latter phases of offshore warmth and subsequent cooling. The pollen taxa indicative of cluster E (Compositae Liguliflorae, deciduous *Quercus*, *Alnus*, Ericaceae) do not easily lend themselves to identification of a particular vegetation community, but the fact that samples belonging to this group recur together through long sections of the sequence supports its identification as a temporally (but not necessarily spatially) distinctive palynological assemblage. Heath vegetation with few trees (cluster B) characterizes the continuation in falling offshore temperatures. Similar heath vegetation, with a small contribution from temperate trees, also developed during MIS 8c. Steppe vegetation (cluster A) increases as the coldest sea surface temperatures prevail once more.

Successive warm stages in the MD01-2443 pollen record are characterized by the same forest taxa, in contrast to existing terrestrial sequences from southern Europe where forests are more diverse and vary in composition from one stage to the next. Typically, for example at Lac du Bouchet, central France, initial pioneer populations of *Juniperus*, *Betula* and *Pinus* are followed by deciduous *Quercus* and *Corylus* but, unlike the Portuguese record, this is followed by other mesic forest trees including *Carpinus*, and then a phase of more montane taxa with greater moisture requirements: *Abies*, *Fagus*, and *Picea* [4,5,59]. It is mainly these trees of the latter part of the succession that vary in abundance between temperate stages [61]. We suggest that the extreme rarity of *Fagus* and *Carpinus* in our sequence is an indication that they did not grow in significant numbers in the MD01-2443 catchment during the temperate intervals of MIS 7 or 9: since *Fagus* is recorded in MIS 7a, 7c, 9c and 9a, and *Carpinus* is present in every temperate interval in marine pollen spectra from Galician margin cores [62] their absence from MD01-2443 is unlikely to be a taphonomic artefact. Either, there was insufficient time during these warm intervals for populations of *Carpinus* and *Fagus* to reach the south-west from their positions of glacial refuge (which may have included north-west Iberia [63–66]), or climatic and/or ecological conditions in the south-west never became favourable.

5.2. Land–sea correlations and stratigraphical implications

While forest expansions are effectively synchronous with shifts in planktonic δ^{18}O, within the resolution of the records, they lag by 1.5–3 ka the mid-points of the shifts in benthic δ^{18}O at transitions from cold to warm intervals. This has stratigraphical implications because it suggests that while land–sea correlations are broadly correct, there may be considerable offsets in the precise timing of terrestrial and marine stage boundaries (defined in terms of vegetation and sea level changes respectively). The extent of this offset may be temporally and spatially variable. Skinner and Shackleton [51] showed, for Termination I, that changes in deep-water hydrography in the Portuguese margin may lead to shifts in the

benthic isotope signal being up to 4 ka earlier than in curves from the eastern equatorial Pacific. Since deep-water hydrography varies from site to site, and from one termination to another, the precise nature of the phase lag between marine and terrestrial stages will vary accordingly. Estimating the local hydrographic component of benthic foraminiferal $\delta^{18}O$ in future would enable a more accurate assessment of phase relationships between marine and terrestrial stage boundaries and would allow the potential status of this sequence as a land–ocean correlation reference scheme for southern Europe to be fully realized. Be that as it may, improved terrestrial chronologies could be still achieved by correlating the onset of forest warm stages with those in the MD01-2443 pollen sequence or, alternatively, by aligning them to cold-to-warm transitions in the planktonic isotope signal.

5.3. Climatic oscillation during deglaciations

Peaks of 40 to 50% *N. pachyderma* s. at TIII and TIV indicate the influence of sub-polar water at the latitude of MD01-2443. These percentages are similar to those encountered in the Heinrich layers of the last glaciation in cores nearby [29,67]. Peaks in ice-rafted detritus (IRD) in these layers record the presence of icebergs off southern Portugal [20,68]. There is currently no lithic record from MD01-2443 but the record from ODP 980 (55°29′N, 14°42′W) in the north-east Atlantic shows distinct peaks in IRD at the deglaciations, including TIII and TIV, suggesting that the peaks in polar foraminifera abundance were related to large iceberg discharges similar to Heinrich events [54]. Smaller peaks in *N. pachyderma* s. abundance indicate lesser, but nonetheless significant, influence of sub-polar water off Portugal and coincide with heavy excursions in planktonic $\delta^{18}O$.

At the deglaciations, TIII and TIV, tree population expansion associated with deglaciation was already under way when it was interrupted by an abrupt drop in sea surface temperature. The cooling appears to have caused reversals in the pattern of tree population expansion. Tree populations then only reached their maximum extent once temperate conditions had returned offshore (and polar foraminifera returned to background levels). The presence of subpolar water, and very likely icebergs, offshore apparently led to cooling and increased aridity downwind in south-west Iberia, which interrupted the warming trend associated with deglaciation. Similar interruptions or pauses are known to have affected this region during the last [9,10] and penultimate [29,69] deglaciations (TI and TII) and have been related to melt-water-induced slowing or cessation of the thermohaline circulation. From our data it seems likely that similar cold events also occurred during TIII and TIV. Interruptions in warming and tree population expansion have also been identified during TIII and TIV in deep sea cores from further north on the Portuguese margin, off Galicia [62, 70]. Higher percentages (up to 90%) of *N. pachyderma* s. reflect the more northerly position of these sites.

5.4. MIS 8 and the timing of TIII

Recent high-precision U-series dates on flowstone from Spannagel Cave (Zillertal Alps, Austria) identified a series of speleothem growth phases during MIS 8 and 7 [71]. In this dataset the earliest interval of calcite deposition occurred between *ca.* 261 and 249 ka, which falls within MIS 8 of the deep-sea stratigraphy [48]. However, Holzkämper et al. [71] considered the possibility that the first growth period of flowstone at 261 ka may reflect an early onset of MIS 7e. This would be in agreement with the U/Th-dated vein calcite record from Devils Hole, Nevada, which shows an increase in $\delta^{18}O$ values around that time and suggests a significantly older age for Termination III [72–74]. These alternatives can now be assessed within the context of the high resolution data from MD01-2443.

The MD01-2443 record shows a warm interval between 249 and 263 ka, characterized by light planktonic $\delta^{18}O$ values, which corresponds approximately to MIS 8c. A similar warm interval is also evident in the Vostok [44] and Dome C [46] records of Antarctic air temperature and has parallels in atmospheric $\delta^{18}O$ and, methane and carbon dioxide concentrations [44]. In all of these records this warm interval is followed by a return to glacial values before the warming associated with deglaciation begins. The MD01-2443 pollen data show an expansion of deciduous *Quercus* populations (MD-14) during MIS 8c, indicating increased warmth and moisture on land. This is followed by a contraction, suggesting cooling and/or aridification, prior to the deglacial tree population expansion. A similar pattern is visible in terrestrial pollen sequences from southern Europe [8,61,75]. In central France, *Pinus* populations expanded [4], as did deciduous *Quercus* and *Pinus* populations in north-west Greece [2] indicating an amelioration of climatic conditions across southern Europe. On the basis of the MD01-2443 and Spannagel cave chronologies the early interval of

speleothem growth, indicating temperatures above freezing at *ca.* 2500 m altitude [71], appears to be correlative with MIS 8c in MD01-2443, within the age uncertainties, which is characterized by increased temperatures, precipitation and tree population expansion. Cessation of speleothem growth marks a drop in temperatures below freezing at 249 ka, which corresponds closely to the pre-termination cooling in MD01-2443 (supporting its placement within MIS 8).

Although the Devils Hole $\delta^{18}O$ dataset [72] is of lower resolution than the marine, terrestrial and ice core sequences discussed here, close inspection reveals considerable structure in the curve at the transition from MIS 8 to 7: an interruption in the warming trend at 254 ka divides the transition into an early period of gradual change and a later period of rapid change. We suggest that the early period of warming is equivalent to the late MIS 8 warm interval (MIS 8c) (Fig. 5), while the minor reversal in the warming trend at 254 ka correlates with the return to glacial values, and the final interval of rapid warming represents the deglaciation. Such an interpretation would mean that the midpoint of the rapid shift in $\delta^{18}O$ at Devils Hole, should be placed later, *ca.* 248 ka. This brings the age of Termination III in this record closer to the MD01-2443, Antarctic and orbital ages for this event, and indeed coincides with these ages when age uncertainties are taken into account.

5.5. The end-MIS 7 sub-orbital oscillation

A sea level high stand has been identified in a $\delta^{18}O$ sequence from the Bahamas [76] and in coral-based sea level estimates from Barbados [58,77] after the peak of MIS 7a (or event 7.1). U–Th dates from these records indicate a discrete high stand lasting 5 to 10 ka after 190 ka, the SPECMAP [7] age for the MIS 7/6 transition [58,76,77] the drop in sea level that marks the onset of the MIS 6 glaciation occurs at the end of this high stand. This additional oscillation at the end of MIS 7 is clearly represented in MD01-2443 where planktonic $\delta^{18}O$ shows a distinct light excursion, suggesting sea surface warming, while benthic $\delta^{18}O$ shows a pause in the trend of increasingly heavy isotopic values. The pollen record shows increased abundance of deciduous *Quercus*, suggesting increased warmth and moisture availability on land. Thus, the sea level high stand, so far only recorded in sea level and marine isotopic records, appears to have also been a period of warmth in south-west Europe. Placing the MIS 7/6 boundary at the mid-point of the isotopic decrease following this extra, sub-orbital scale oscillation (rather than following the first MIS 7a peak [13]) gives an age of 184 ka in our chronology. This is broadly in line, when age uncertainties are taken into account, with the maximum age of 180 ka, suggested by [76] and [77], for the end of the high stand.

6. Conclusions

1. MD01-2443 records similar patterns of ocean surface conditions and forest extent at orbital and millennial time scales, indicating a spatial coherence of climate variability between the North Atlantic and south-west Europe with an ocean-atmosphere linkage.
2. Each precessional cycle is characterized by a similar succession of vegetation types: i) pioneer populations with abundant *Juniperus*, ii) temperate tree populations dominated by deciduous *Quercus*, iii) ericaceous heathland, and iv) steppe vegetation, closely following the pattern of warming and cooling recorded offshore.
3. Heinrich-type events, leading to incursions of subpolar water at the site, during deglaciations (TIII and TIV) appear to have caused cooling and increased aridity in Portugal: tree population expansion was interrupted by brief reversals coincident with the arrival of subpolar water masses.
4. The close relationship, in timing and in amplitude, between sea surface conditions and forest extent breaks down in MIS 9e and 7e. Forest collapse, indicating pronounced cooling and aridification on land, early on in these marine isotopic substages appears to coincide with cooling and decreasing atmospheric methane concentrations recorded in Antarctic ice cores, pointing to a global scale climatic shift. However, there is no accompanying change in water masses at the Portuguese margin or further north.
5. The high-resolution MD01-2443 record shows that the most extreme glacial conditions of MIS 8 occurred during the first part (MIS 8d), culminating in a Heinrich-type event. This was followed by an interval of warmer conditions and tree population expansion (MIS 8c), and then a return to glacial values before TIII. This suggests that previous claims for an early deglaciation based on lower-resolution records have been conflating the onset of MIS 8c with TIII. The sub-orbital scale sea level high stand identified recently at the end of MIS 7 is recognised in MD01-2443 as a (double) light peak in the planktonic isotope curve and corresponding

expansion of deciduous *Quercus* populations, indicating warmth in south-west Iberia.

6. The data show offsets in the timing of benthic isotopic and palynological changes, underlining the value of marine pollen records in land–ocean correlation. The precise temporal relationship between forest expansion and deglaciation depends on identification of the local hydrographic component in the benthic isotope record in the future.

Acknowledgements

This work was funded by the "POP Project", EC Grant EVK2-2000-00089 and NERC grant NER/A/S/2002/00946. Funding for L.A. was provided by the Portuguese Foundation for Science and Technology under the fellowship contract: SFRH/BPD/1588/2000 and by the Calouste Gulbenkian Foundation, through a visiting fellowship to Woods Hole Oceanographic Institution. We are grateful to the French MENRT, TAAF, CNRS/INSU and especially to IFRTP for the coring operations aboard the Marion Dufresne II. We thank M. Hall for isotopic measurements, I. Lawson and O. Philips for comments on the manuscript, and A. Mangini and F. Bassinot for helpful reviews. We dedicate this paper to the memory of our co-author Nick Shackleton, our colleague, mentor and friend.

References

[1] T.A. Wijmstra, Palynology of first 30 metres of a 120 m deep section in Northern Greece, Acta Bot. Neerl. 18 (1969) 511–527.

[2] T.A. Wijmstra, A. Smit, Palynology of middle part 30–78 meters of 120 m deep section in northern Greece Macedonia, Acta Bot. Neerl. 25 (1976) 297–312.

[3] M. Follieri, D. Magri, L. Sadori, 250,000-year pollen record from Valle di Castiglione Roma, Pollen Spores 30 (1988) 329–356.

[4] M. Reille, V. Andieu, J-L. Beaulieu, P. Guenet, C. Goeury, A long pollen record from Lac du Bouchet, Massif Central, France: for the period ca. 325 to 100 ka BP OIS 9c to OIS 9e, Quat. Sci. Rev. 17 (1998) 107–1123.

[5] M. Reille, J-L. de Beaulieu, Long Pleistocene pollen records from the Praclaux crater, South-Central France, Quat. Res. 44 (1995) 205–215.

[6] W.L. Prell, J. Imbrie, D.G. Martinson, J. Morley, N.G. Pisias, N.J. Shackleton, H.F. Streeter, Graphic correlation of oxygen isotope stratigraphy application to the late Quaternary, Paleoceanography 1 (1986) 137–162.

[7] D.G. Martinson, N.G. Pisias, J.D. Hays, J. Imbrie, T.C. Moore, N.J. Shackleton, Age dating and the orbital theory of the ice ages — development of a high-resolution-0 to 300,000-year chronostratigraphy, Quat. Res. 27 (1987) 1–29.

[8] P.C. Tzedakis, V. Andrieu, J.L. deBeaulieu, S. Crowhurst, M. Follieri, H. Hooghiemstra, D. Magri, M. Reille, L. Sadori, N.J. Shackleton, W. Ta, Comparison of terrestrial and marine records of changing climate of the last 500,000 years, Earth Planet. Sci. Lett. 150 (1997) 171–176.

[9] N.J. Shackleton, M. Chapman, M.F. Sánchez Goñi, D. Pailer, Y. Lancelot, The classic marine isotope substage 5e, Quat. Res. 58 (2002) 14–16.

[10] M.F. Sánchez Goñi, F. Eynaud, J.-L. Turon, N.J. Shackleton, High resolution palynological record off the Iberian margin: direct land–sea correlation for the last interglacial complex, Earth Planet. Sci. Lett. 171 (1999) 123–137.

[11] N.J. Shackleton, M.F. Sánchez Goñi, D. Pailler, Y. Lancelot, Marine isotope stage 5e and the Eemian interglacial, Glob. Planet. Change 36 (2003) 151–155.

[12] K.H. Roucoux, L. de Abreu, N.J. Shackleton, P.C. Tzedakis, The response of NW Iberian vegetation to North Atlantic climate oscillations during the last 65 kyr, Quat. Sci. Rev. 24 (2005) 1637–1653.

[13] P.C. Tzedakis, K.H. Roucoux, L. de Abreu, N.J. Shackleton, The duration of forest stages in southern Europe and interglacial climate variability, Science 306 (2004) 2231–2235.

[14] L. de Abreu, F.F. Abrantes, N.J. Shackleton, P.C. Tzedakis, J.F. McManus, D.W. Oppo, M.A. Hall, Ocean climate variability in the Eastern North Atlantic during interglacial MIS 11: a partial analogue to the Holocene? Paleoceanography 20 (2005) PA3009, 30, doi:10.1029/2004PA001091.

[15] G. Dietrich, K. Kalle, W. Krauss, G. Siedler, General oceanography, John Wiley and Sons Inc., Chichester, 1980, 626 pp.

[16] A.F.G. Fiuza, M. Hamann, I. Ambar, G.D. del Rio, N. Gonzalez, J.M. Cabanas, Water masses and their circulation off western Iberia during May 1993, Deep-Sea Res., Part 1, Oceanogr. Res. Pap. 45 (1998) 1127–1160.

[17] W.F. Ruddiman, A. McIntyre, The North-Atlantic Ocean during the last deglaciation, Palaeogeogr. Palaeoclimatol. Palaeoecol. 35 (1981) 145–214.

[18] O. Cayre, Y. Lancelot, E. Vincent, M. Hall, Palaeoceanographic reconstructions from planktonic foraminifers off the Iberian margin: temperature, salinity and Heinrich events, Paleoceanography 14 (1999) 384–396.

[19] S.M. Lebreiro, J.C. Moreno, I.N. McCave, P.P.E. Weaver, Evidence for Heinrich layers off Portugal (Tore Seamount: 39 degrees N, 12 degrees W), Mar. Geol. 131 (1996) 47–56.

[20] J.H. Baas, J. Mienert, F. Abrantes, M.A. Prins, Late Quaternary sedimentation on the Portuguese continental margin: Climate-related processes and products, Palaeogeogr. Palaeoclimatol. Palaeoecol. 130 (1997) 1–23.

[21] L.E. Heusser, Pollen distribution in marine sediments on the continental margin off northern California, Mar. Geol. 80 (1988) 131–147.

[22] G.L. Chmura, A. Smirnov, I.D. Campbell, Pollen transport through distributaries and depositional patterns in coastal waters, Palaeogeogr. Palaeoclimatol. Palaeoecol. 149 (1999) 257–270.

[23] R. Cheddadi, H.F. Lamb, J. Guiot, S. van der Kaars, Holocene climatic change in Morocco: a quantitative reconstruction from pollen data, Clim. Dyn. 14 (1998) 883–890.

[24] K.H. Roucoux, N.J. Shackleton, J. Schönfeld, P.C. Tzedakis, Combined marine proxy and pollen analyses reveal rapid Iberian vegetation response to North Atlantic millennial-scale climate oscillations, Quat. Res. 56 (2001) 128–132.

[25] M.F. Sánchez Goñi, J.-L. Turon, F. Eynaud, S. Gendreau, European climatic response to millennial-scale changes in the atmosphere-ocean system during the last glacial period, Quat. Res. 54 (2000) 394–403.

[26] W.O. van der Knaap, J.F.N. van Leeuwen, Late Glacial and early Holocene vegetation succession, altitudinal zonation, and climate change in the Serra da Estrela, Portugal, Rev. Palaeobot. Palynol. 97 (1997) 239–285.
[27] P.J. Mudie, F.G. McCarthy, Late Quaternary pollen transport processes, western North Atlantic: data from box models, cross-margin and N–S transects, Mar. Geol. 118 (1994) 79–105.
[28] K.H. Roucoux, Millennial scale vegetation and climate variability in north-west Iberia during the last glacial stage, PhD, University of Cambridge, 2000.
[29] J.-L. Turon, A.-M. Lézine, M. Denèfle, Land–sea correlations for the last glaciation inferred from a pollen and dinocyst record from the Portuguese margin, Quat. Res. 59 (2003) 88–96.
[30] C.C. Wallén, World Survey of Climatology, vol. 5: Climates of Northern and Western Europe, Elsevier, Amsterdam, 1970, 253 pp.
[31] O. Polunin, B.E. Smythies, Flowers of South-West Europe, a field guide, Oxford University Press, Oxford, UK, 1997, 480 pp.
[32] O. Polunin, M. Walters, A guide to the vegetation of Britain and Europe, Oxford University Press, Oxford, UK, 1985, 238 pp.
[33] W.O. van der Knaap, J.F.N. van Leeuwen, Holocene vegetation succession and degradation responses to climatic change and human activity in the Serra da Estrela, Portugal, Rev. Palaeobot. Palynol. 89 (1995) 153–211.
[34] N.J. Shackleton, Attainment of isotopic equilibrium between ocean water and the benthic foraminifera genus *Uvigerina*: isotopic changes in the ocean during the last glacial, Cent. Natl. Rech. Sci. Coll. Int. 219 (1974) 203–209.
[35] J.P. Kennett, M.S. Srinivasan, Neogene Planktonic Foraminifera. A phylogenetic atlas, Hutchinson Ross Publishing Company, 1983, 265 pp.
[36] A.R. Loeblich Jr., H. Tappan, in: R.C. Moore (Ed.), Treatise on Invertebrate Paleontology, part C: Protista 2, Geological Society of America, University of Kansas Press, 1988, pp. 511–900.
[37] B.E. Berglund, M. Ralska-Jasiewiczowa, Pollen analysis and pollen diagrams, in: B.E. Berglund (Ed.), Handbook of Holocene Palaeoecology and Palaeohydrology, John Wiley and Sons Inc., Chichester, 1986, pp. 455–484.
[38] M. Reille, Pollen et spores d'Europe et d'Afrique du Nord, Laboratoire de Botanique Historique et Palynologie, Marseille, France, 1992, 520 pp.
[39] T.G. Tutin, N.A. Burges, A.O. Chater, J.R. Edmonson, V.H. Heywood, D.M. Moore, D.H. Valentine, S.M. Walters, D.A. Webb, Flora Europaea, vol. 1–5, Cambridge University Press, Cambridge, UK, 1980.
[40] J. Mateus, Holocene and present-day ecosystems of the Carvalhal Region, southwest Portugal, PhD, University of Utrecht, 1992, 183 pp.
[41] B. McCune, M.J. Mefford, PC-ord. Multivariate Analysis of Ecological Data, Version 4, MjMSoftware Design, Gleneden Beach, Oregon, USA, 1999.
[42] M. Dufrene, P. Legendre, Species assemblages and indicator species: the need for a flexible asymmetrical approach, Ecol. Monogr. 67 (1997) 345–366.
[43] K. Faegri, J. Iversen, Textbook of Pollen Analysis, Blackwell Scientific Publications Ltd., Oxford, 1975 295 pp.
[44] J.R. Petit, J. Jouzel, D. Raynaud, N.I. Barkov, J.M. Barnola, I. Basile, M. Bender, J. Chappellaz, M. Davis, G. Delaygue, M. Delmotte, V.M. Kotlyakov, V.Y. Lipenkov, M. Legrand, C. Lorius, L. Pepin, C. Ritz, E.S. Saltzman, M. Stievenard, Climate and atmospheric history of the past 420,000 years from the Vostok ice core, Antarctica, Nature 399 (1999) 429–436.
[45] N.J. Shackleton, M.A. Hall, E. Vincent, Phase relationships between millennial-scale events 64,000–24,000 years ago, Paleoceanography 15 (2000) 565–569.
[46] EPICA Community Members, Eight glacial cycles from an Antarctic ice core, Nature 429 (2004) 623–628.
[47] W.S. Broecker, J. van Donk, Insolation changes, ice volumes, and O-18 record in deep-sea cores, Rev. Geophys. Space Phys. 8 (1970) 169–198.
[48] F.C. Bassinot, L.D. Labeyrie, E. Vincent, X. Quidelleur, N.J. Shackleton, Y. Lancelot, The astronomical theory of climate and the age of the Brunhes–Matuyama magnetic reversal, Earth Planet. Sci. Lett. 126 (1994) 91–108.
[49] L. de Abreu, High resolution palaeoceanography off Portugal during the last two glacial cycles, PhD, University of Cambridge, 2000, 366 pp.
[50] L. de Abreu, Millennial-scale oceanic climate variability off the Western Iberian margin during the last two glacial periods, Mar. Geol. 196 (2003) 1–20.
[51] L.C. Skinner, N.J. Shackleton, An Atlantic lead over Pacific deep-water change across Termination I: implications for the application of the marine isotope stratigraphy, Quat. Sci. Rev. 24 (2005) 571–580.
[52] A. Berger, Long term variations of caloric insolation resulting from the Earth's orbital elements, Quat. Res. 9 (1978) 139–167.
[53] W.F. Ruddiman, A. McIntyre, Severity and speed of Northern Hemisphere glaciation pulses — the limiting case, Geol. Soc. Amer. Bull. 93 (1982) 1273–1279.
[54] J.F. McManus, D.W. Oppo, J.L. Cullen, A 0.5-million-year record of millennial-scale climate variability in the North Atlantic, Science 283 (1999) 971–975.
[55] N.J. Shackleton, The 100,000-year ice-age cycle identified and found to lag temperature, carbon dioxide and orbital eccentricity, Science 289 (2000) 1897–1902.
[56] C. Waelbroeck, L. Labeyrie, E. Michel, J.C. Duplessy, J.F. McManus, K. Lambeck, E. Balbon, M. Labracherie, Sea-level and deep water temperature changes derived from benthic foraminifera isotopic records, Quat. Sci. Rev. 21 (2001) 295–305.
[57] C.H. Stirling, T.M. Esat, K. Lambeck, M.T. McCulloch, S.G. Blake, D.-C. Lee, A.N. Halliday, Orbital forcing of the marine isotope stage 9 interglacial, Science 291 (2001) 290–293.
[58] W.G. Thompson, S.L. Goldstein, Open-system coral ages reveal persistent suborbital sea-level cycles, Science 308 (2005) 401–404.
[59] M. Reille, J-L. de Beaulieu, H. Svobodova, V. Andieu-Ponel, C. Goeury, Pollen analytical biostratigraphy of the last five climatic cycles from a long continental sequence from the Velay region Massif Central, France, J. Quat. Sci. 15 (2000) 665–685.
[60] Shipboard data: MD123 Geosciences, Leg 2 (2001).
[61] P.C. Tzedakis, Establishing a terrestrial chronological framework as a basis for biostratigraphical comparisons, Quat. Sci. Rev. 20 (2001) 1583–1592.
[62] S. Desprat, M.F. Sánchez Goñi, J.-L. Turon, J. Duprat, B. Malaizé, J.-P. Peypouquet, Climatic variability of Marine Isotope Stage 7: direct land–sea–ice correlation from a multiproxy analysis of a northwestern Iberian margin deep-sea core, Quat. Sci. Rev. 25 (2006) 1010–1026.

[63] P. Ramil-Rego, C. Munoz-Sobrino, M. Rodriguez-Guitian, L. Gomez-Orellana, Differences in the vegetation of the North Iberian Peninsula during the last 16,000 years, Plant Ecol. 138 (1998) 41–62.

[64] P. Ramil-Rego, M.A.R. Guitian, C.M. Sobrino, L. Gomez-Orellana, Some considerations about the postglacial history and recent distribution of *Fagus sylvatica* in the NW Iberian Peninsula, Folia Geobot. 35 (2000) 241–271.

[65] C.M. Sobrino, P. Ramil-Rego, M.R. Guitian, Upland vegetation in the north-west Iberian peninsula after the last glaciation: forest history and deforestation dynamics, Veg. Hist. Archaeobot. 6 (1997) 215–233.

[66] C.M. Sobrino, P. Ramil-Rego, L. Gomez-Orellana, Vegetation of the Lago de Sanabria area (NW Iberia) since the end of the Pleistocene: a palaeoecological reconstruction on the basis of two new pollen sequences, Veg. Hist. Archaeobot. 13 (2004) 1–22.

[67] M.F. Sánchez Goñi, I. Cacho, J.-L. Turon, J. Guiot, F.J. Sierro, J.-P. Paypouquet, J.O. Grimalt, N.J. Shackleton, Synchroneity between marine and terrestrial responses to millennial scale climatic variability during the last glacial period in the Mediterranean region, Clim. Dyn. 19 (2002) 95–105.

[68] E. Cortijo, L. Labeyrie, L. Vidal, M. Vautravers, M. Chapman, J.C. Duplessy, M. Elliot, M. Arnold, J.L. Turon, G. Auffret, Changes in sea surface hydrology associated with Heinrich event 4 in the North Atlantic Ocean between 40 degrees and 60 degrees N, Earth Planet. Sci. Lett. 146 (1997) 29–45.

[69] E. Bard, F. Rostek, J.L. Turon, S. Gendreau, Hydrological impact of Heinrich events in the subtropical northeast Atlantic, Science 289 (2000) 1321–1324.

[70] S. Desprat, M.F. Sánchez Goñi, J.-L. Turon, J. Duprat, B. Malaizé, J.-P. Peypouquet, Climate variability of the last five isotopic interglacials from direct land–sea–ice correlation, in: F. Sirocko, M. Claussen, T. Litt, M.F. Sanchez-Goni, (Eds), The climate of past interglacials, Developments in Quaternary Sciences, Elsevier, in press.

[71] S. Holzkämper, C. Spötl, A. Mangini, High-precision constraints on timing of Alpine warm periods during the middle to late Pleistocene using speleothem growth periods, Earth Planet. Sci. Lett. 236 (2005) 751–764.

[72] I.J. Winograd, J.M. Landwehr, K.R. Ludwig, T.B. Coplen, A.C. Riggs, Duration and structure of the past four interglaciations, Quat. Res. 48 (1997) 141–154.

[73] C.D. Gallup, H. Cheng, F.W. Taylor, R.L. Edwards, Direct determination of the timing of sea level change during termination, Science 295 (2002) 310–313.

[74] I.J. Winograd, T.B. Coplen, J.M. Landwehr, A.C. Riggs, K.R. Ludwig, B.J. Szabo, P.T. Kolesar, K.M. Revesz, Continuous 500,000-year climate record from vein Calcite in Devils–Hole, Nevada, Science 258 (1992) 255–260.

[75] K.H. Roucoux, P.C. Tzedakis, L. de Abreu, N.J. Shackleton, Fine tuning land–ocean correlations for the Middle Pleistocene of southern Europe, in: F. Sirocko, M. Claussen, T. Litt, M.F. Sanchez-Goni, (Eds), The Climate of Past Interglacials, Devlopments in Quaternary Sciences, Elsevier, in press.

[76] G.M. Henderson, L.F. Robinson, K. Cox, A.L. Thomas, Recognition of non-Milankovitch sea-level highstands at 185 and 343 thousand years ago from U–Th dating of Bahamas sediment, Quat. Sci. Rev. (in press).

[77] W.G. Thompson, S.L. Goldstein, A radiometric calibration of the SPECMAP time scale, Quat. Sci. Rev. (in press).